

Exponentially Damped Lévy Flights, Multiscaling, and Exchange Rates

Raul Matsushita^a, Iram Gleria^b, Annibal Figueiredo^c, Pushpa Rathie^a,
Sergio Da Silva^{d*}

^a*Department of Statistics, University of Brasilia, 70910-900 Brasilia DF, Brazil*

^b*Department of Physics, Federal University of Alagoas, 57072-970, Maceio AL, Brazil*

^c*Department of Physics, University of Brasilia, 70910-900 Brasilia DF, Brazil*

^d*Department of Economics, Federal University of Rio Grande Do Sul, 90040-000 Porto Alegre
RS, Brazil*

Abstract

We employ our previously suggested exponentially damped Lévy flight [14] to study the multiscaling properties of 30 daily exchange rates against the US dollar together with a fictitious euro-dollar rate [16]. Though multiscaling is not theoretically seen in either stable Lévy processes or abruptly truncated Lévy flights, it is even characteristic of smoothly truncated Lévy flights [11, 15]. We have already defined a class of "quasi-stable" processes in connection with the finding that single scaling is pervasive among the dollar price of foreign currencies [8]. Here we show that the same goes as far as multiscaling is concerned. Our novel findings incidentally reinforce the case for real-world relevance of the Lévy flights for modeling financial prices.

PACS: 05.40.+j;02.50.-r

Keywords: Lévy distributions; foreign exchange rates; multiscaling

1. Introduction

Financial prices are unlikely to follow Gaussian random walks [1]. Returns are larger than expected by Gaussian assumptions. Financial markets are also likely to be governed by random Lévy processes.

Ordinary Lévy distributions [2, 3] are stable and have fat power-law tails that decay more slowly than an exponential decay. This feature can track extreme events, and that is plausible. But it also leads to an infinite variance, which is implausible.

Modifications to the ordinary Lévy distribution have been suggested in literature as an attempt to overturn such a drawback. They were pioneered by Mantegna and Stanley [4], who carried out an abrupt truncation on the original distribution tails. A canonical example of the use of the truncated Lévy flight (TLF) for real-world financial data is that of Mantegna and Stanley for the S&P500 [5]. Their approach has since been employed and extended to other asset prices [6, 7, 8, 9]. With finite data sets the TLF is not stable though, but has finite variance and slowly converges to a Gaussian equilibrium as implied by the central limit theorem.

* Corresponding author.

E-mail address: SergioDaSilva@angelfire.com (S. Da Silva)

Owing to the sharp truncation, the characteristic function of the TLF is no longer infinitely divisible as well. However, it is still possible to define a TLF with a smooth cutoff that yields an infinitely divisible characteristic function [10]. This has been dubbed a smoothly truncated Lévy flight (STLF). In such a case, the cutoff is carried out by asymptotic approximation of a stable distribution valid for large values [11].

Yet the STLF breaks down in the presence of positive feedbacks [12, 13]. But the cutoff can still be alternatively combined with a statistical distribution factor to generate a gradually truncated Lévy flight (GTLF) [12, 13]. Nevertheless that procedure also brings fatter tails. The GTLF itself also breaks down if the positive feedbacks are strong enough. This apparently happens because the truncation function decreases exponentially.

Generally the sharp cutoff of the TLF makes moment scaling approximate and valid for a finite time interval only; for longer time horizons, scaling must break down. And the breakdown depends not only on time but also on moment order.

An exponentially damped Lévy flight (EDLF) which encompasses all the previous cases has been suggested [14] by some of us exactly because a distribution might be assumed to deviate from the Lévy in both a smooth and gradual fashion in the presence of positive feedbacks that may increase.

Whether scaling is single or multiple depends on how a Lévy flight is broken. While the abruptly truncated Lévy flight (the TLF itself) exhibits mere single scaling, the STLF shows multiscaling [11, 15]. Some of us have first employed an abruptly TLF [8] to fit data for daily exchange rates against the US; and we then realized that the same data set might be well fitted by an EDLF [14].

Here we move up and focus on the multiscaling properties stemming from the EDLF. We thus evaluate the multiscaling properties of the same 30 daily exchange rates against the dollar. We also add a *false* euro [16] to our data sets. We find multiscaling to be pervasive among these. We also connect the class of "quasi-stable" processes defined previously by some of us [8] with multiscaling. This paper thus presents novel theoretical results together with an analysis of actual exchange rates. The paper then adds to the previous literature on multiscaling and exchange rates [17-22].

The structure of the paper is as follows. Section 2 presents the truncated variants of the Lévy distribution, including our previously defined EDLF. Section 3 deals with the multiscaling properties of the EDLF, and Section 4 links the class of quasi-stable processes with multiscaling behavior. Section 5 exemplifies with actual exchange rates, and Section 6 concludes.

2. The ordinary Lévy distribution and its truncated variants

To begin with, let S_n be the sum of n independent and identically distributed random variables X_t ,

$$S_n = X_1 + X_2 + X_3 \dots + X_n \quad (1)$$

with $E(X_t) = 0$. A usual attitude in finance is to work with returns, i.e.

$$Z_{\Delta t}(t) = S_t - S_{t-\Delta t} = X_t + X_{t-1} + \dots + X_{t-\Delta t+1} \quad (2)$$

where Δt is a time lag. Now consider the symmetric Lévy distribution

$$L(Z_{\Delta t}) \equiv \frac{1}{\pi} \int_0^{\infty} \exp(-\gamma \Delta t q^\alpha) \cos(q Z_{\Delta t}) dq \quad (3)$$

where $0 < \alpha < 2$, and $\gamma > 0$ is a scale factor.

The characteristic function of (3), $\varphi(K)$, is such that

$$\ln[\varphi(K)] = -\gamma\Delta t|K|^\alpha \quad (4)$$

which satisfies $\Delta t \ln[\varphi(K)] = \ln[\varphi(\Delta t^{1/\alpha} K)]$. This means that the corresponding probability distribution is

$$L(Z_{\Delta t}) = \Delta t^{-1/\alpha} L(\Delta t^{-1/\alpha} Z_{\Delta t}) = \Delta t^{-1/\alpha} L(Z_s) \quad (5)$$

where $Z_s = \Delta t^{-1/\alpha} Z_{\Delta t}$ is a scaled variable at Δt .

Let us define a modified Lévy flight (MLF) through

$$P(Z_{\Delta t}) = \eta L(Z_{\Delta t}) f(Z_{\Delta t}) \quad (6)$$

where η is a normalizing constant, and $f(Z_{\Delta t})$ is the change carried out on the distribution.

The abruptly truncated Lévy flight (TLF) is an extension to which

$$f(Z_{\Delta t}) = f_{\text{abrupt}}(Z_{\Delta t}) = \begin{cases} 0, & (|Z_{\Delta t}| > l_{\max}) \\ 1, & (|Z_{\Delta t}| \leq l_{\max}) \end{cases} \quad (7)$$

where l_{\max} is the step size at which the distribution begins to depart from the ordinary Lévy. The TLF is not stable and has finite variance; therefore it converges to a Gaussian equilibrium according the central limit theorem. The characteristic function of the TLF is no longer infinitely divisible. Nevertheless approximate scaling can still occur for a finite time interval [23]. But scaling must break down for longer time intervals.

We then consider the smoothly truncated Lévy flight (STLF) [10, 11]. The cutoff parameter $\lambda_0 > 0$ is now introduced into Eq. (6) as

$$f(Z_{\Delta t}) = f_{\text{smooth}}(Z_{\Delta t}) = \begin{cases} Ca |Z_{\Delta t}|^{-1-\alpha} e^{-\lambda_0|Z_{\Delta t}|}, & (Z_{\Delta t} < 0) \\ Cb Z_{\Delta t}^{-1-\alpha} e^{-\lambda_0 Z_{\Delta t}}, & (Z_{\Delta t} > 0) \end{cases} \quad (8)$$

Function $f_{\text{smooth}}(Z_{\Delta t})$ is based on the asymptotic approximation of a stable distribution of index α valid for large values of $|Z_{\Delta t}|$ when $\gamma = 1$. It exhibits a power law behavior. For $0 < \alpha < 1$, the first term of the expansion of $L(Z_{\Delta t})$ can be approximated by

$$L(Z_{\Delta t}) \approx \frac{\gamma\Delta t\Gamma(1+\alpha)\sin(\pi\alpha/2)|Z_{\Delta t}|^{-(1+\alpha)}}{\pi} \quad (9)$$

By taking into account the particular case of the Lévy where $a = b$, we get

$$\ln[\varphi_{\text{STLF}}(K)] = \begin{cases} \gamma\{(\lambda_0^2 + K^2)^{\alpha/2} \cos(\alpha\theta) - \lambda_0^\alpha\}, & (0 < \alpha < 1) \\ \gamma\lambda_0^\alpha\{(1 + iK/\lambda_0)^\alpha - 1\}, & (1 < \alpha < 2) \end{cases} \quad (10)$$

where $\theta = \arctan(K/\lambda_0)$, and $\gamma = C\Gamma(-\alpha)$. Now the characteristic function ends up infinitely divisible. The convolutions of its corresponding distribution can be collapsed onto $\Delta t = 1$ by scaling $Z_{\Delta t}$ and λ_0 . By considering (6), (8), and (9), the approximate variance of the STLF obtains, i.e.

$$\sigma_{\text{smooth}}^2 = \Delta t^{2/\alpha} 2\eta\gamma\pi^{-1}\Gamma(1+\alpha)\sin(\pi\alpha/2)\lambda_s^{\alpha-2}\Gamma(2-\alpha) \quad (11)$$

where $\lambda_s = \Delta t^{1/\alpha}\lambda_0$ is the scaled value of λ_0 .

Finally the gradually truncated Lévy flight (GTLF) [12, 13] is defined as

$$f(Z_{\Delta t}) = f_{\text{gradual}}(Z_{\Delta t}) = \begin{cases} 1, & (|Z_{\Delta t}| \leq l_c) \\ \exp\left[-\left(\frac{|Z_{\Delta t}| - l_c}{\beta_1}\right)^{\beta_0}\right], & (|Z_{\Delta t}| > l_c) \end{cases} \quad (12)$$

where l_c is the step size at which the distribution starts to deviate from the Lévy. Here β_0 and β_1 are the constants related to the truncation. By taking (6), (9), and (12) into account, the approximate variance is now given by

$$\sigma_{gradual}^2 = \frac{\Delta t^{2/\alpha} 2\eta\gamma\Gamma(1+\alpha)\sin(\pi\alpha/2)}{\pi(2-\alpha)} O_{gradual} \quad (13)$$

where

$$O_{gradual} = l_s^{2-\alpha} + (2-\alpha) \left(l_s + \frac{\beta_s \Gamma(2/\beta_0)}{\Gamma(1/\beta_0)} \right)^{1-\alpha} \frac{\beta_s}{\beta_0} \Gamma(1/\beta_0) \quad (14)$$

with $\beta_0 \neq 1$, $l_s = \Delta t^{-1/\alpha} l_c$, and $\beta_s = \Delta t^{-1/\alpha} \beta_1$.

Elsewhere [8] some of us have dealt with the currency data also presented here only to realize that their distributions deviate from the Lévy in a smooth and gradual fashion after $|Z_{\Delta t}| > l_c$. Sometimes the deviations were also caught increasing. Such class of deviations was already found to be positive [12, 13], which means even fatter tails. It has been argued [12, 13] that, since the physical capacity of a system is limited, the feedback begins to decrease exponentially (and not abruptly) after a certain critical step size. In contrast, in the presence of our previously found increasing deviations, we argue that an abrupt truncation is necessary still. In such cases, using the truncation approaches as in Eqs. (7), (8), and (12) might prove not to be appropriate.

For this very reason some of us have already suggested [14] a broader formulation for $f(Z_{\Delta t})$ dubbed exponentially damped Lévy flight (EDLF). The EDLF encompasses the previous TLF, STLF, and GTLF. The EDLF is defined as

$$f(Z_{\Delta t}) = f_{damped}(Z_{\Delta t}) = \begin{cases} 1, & |Z_{\Delta t}| < l_c \\ (\Delta t^{-1/\alpha} |Z_{\Delta t}| + \mathcal{G})^{\tau_1} \exp\{H(Z_{\Delta t})\}, & (l_c < |Z_{\Delta t}| < l_{max}) \\ 0, & |Z_{\Delta t}| > l_{max} \end{cases} \quad (15)$$

where

$$H(Z_{\Delta t}) = \lambda_1 + \lambda_2 [1 - |Z_{\Delta t}|/l_{max}]^{\tau_2} + \lambda_3 (|Z_{\Delta t}| - l_c)^{\tau_3} \quad (16)$$

and \mathcal{G} , λ_1 , $\lambda_2 \leq 0$, $\lambda_3 \leq 0$, τ_1 , τ_2 , and τ_3 are parameters describing the deviations from the Lévy, l_c is (as before) the step size at which the distribution begins to deviate from the Lévy, and l_{max} is the step size at which an abrupt truncation is carried out.

Note that when $l_{max} \rightarrow \infty$, we have

$$H(Z_{\Delta t}) = \lambda_1 + \lambda_2 + \lambda_3 (|Z_{\Delta t}| - l_c)^{\tau_3} \quad (17)$$

By setting $\mathcal{G} = 0$, $\tau_1 = -1 - \alpha$, $l_c = 0$, and $\tau_3 = 1$ in Eqs. (15), (16), and (17), the resulting function is thus equivalent to the smooth case given by Eq. (8). When $l_{max} \rightarrow \infty$, the similar function for the gradual case can be found by setting $\mathcal{G} = \lambda_1 = \lambda_2 = \tau_1 = 0$. The abrupt case is given by setting $l_c = 0$ and choosing the appropriate parameters such that $H(Z_{\Delta t}) \rightarrow -\infty$. By using (6), (9), and (15), and considering the case with l_{max} finite, $\mathcal{G} = 0$, and $\lambda_3 = 0$, the approximate variance is given by

$$\sigma_{damped}^2 = \frac{\Delta t^{2/\alpha} 2\eta\gamma\Gamma(1+\alpha)\sin(\pi\alpha/2)}{\pi} O_{Damped} \quad (18)$$

where

$$O_{Damped} = \frac{l_{cs}^{(2-\alpha)}}{2-\alpha} + l_{ms}^{2-\alpha+\tau_1} e^{\lambda_1} \sum_{j \geq 0} \frac{\lambda_2^j}{j!} B_u(1+j\tau_2, 2-\alpha+\tau_1) \quad (19)$$

$l_{ms} = \Delta t^{-1/\alpha} l_{max}$, $l_{cs} = \Delta t^{-1/\alpha} l_c$, and $B_u(1+j\tau_2, 2-\alpha+\tau_1)$ is the incomplete Beta function with $1+j\tau_2 > 0$, $2-\alpha+\tau_1 > 0$, and $u = 1 - l_c/l_{max}$.

It is worth noting that expressions (11), (13), and (18) all exhibit power laws of type $\sigma_{\Delta t}^2 = \nu \Delta t^{2/\alpha}$, where ν is a constant describing the ‘‘quasi-stable’’ processes that emerge from the truncation parameters for some interval $\Delta t_1 \leq \Delta t \leq \Delta t_2$. Quasi-stable

processes were previously suggested by some of us [8] and will be revisited in Section 4.

3. Power laws

By scaling $Z_{\Delta t}$ together with the truncation parameters, a distribution can be collapsed onto $\Delta t = 1$. We thus have

$$P(Z_{\Delta t}) = \eta L(Z_{\Delta t}) f(Z_{\Delta t}) = \Delta t^{-1/\alpha} \eta L(Z_s) f_s(Z_s) = \Delta t^{-1/\alpha} P_s(Z_s) \quad (20)$$

where $Z_s = \Delta t^{-1/\alpha} Z_{\Delta t}$, and $f_s(Z_s)$ is a truncation function defined by the scaled parameters $l_{ms} = \Delta t^{-1/\alpha} l_{\max}$, $l_{cs} = \Delta t^{-1/\alpha} l_c$, and $\lambda_{3s} = \Delta t^{\tau_3/\alpha} \lambda_3$.

Power laws for both the K^{th} absolute moment and norm of the characteristic function of the EDLF can now be derived. By scaling $Z_{\Delta t}$ and using $l_{ms} = \Delta t^{-1/\alpha} l_{\max}$, $l_{cs} = \Delta t^{-1/\alpha} l_c$, and $\lambda_{3s} = \Delta t^{\tau_3/\alpha} \lambda_3$, the K^{th} absolute moment $E[|Z_{\Delta t}|^K]$ can be reckoned as

$$E[|Z_{\Delta t}|^K] = \Delta t^{K/\alpha} E_s[|Z_s|^K] \quad (21)$$

Note that such a power law depends on α and l_{\max} , l_c , and λ_3 . If it were dependent only on α , multiscaling could not emerge because $\ln E[|Z_{\Delta t}|^K]$ would be given by a linear function K/α .

Now let $\langle |Z_{\Delta t}(t)|^K \rangle = \frac{1}{n} \sum_{t=1}^n |S_t - S_{t-\Delta t}|^K$, and $\langle |\tilde{Z}|^K \rangle = \frac{1}{n} \sum_{t=1}^n |S_t - S_{t-1}|^K$ be the K^{th} sample mean of the lagged absolute values of S_t at the time interval Δt and 1 respectively. For moments which are low enough (such as $0 < K < \alpha$), $P(Z_{\Delta t})$ is expected to be approximated by $L(Z_{\Delta t})$, which in turn does not depend on the truncation parameters [11]. The reason why this might occur is that tails differ, and thereby they do not contribute a great deal to the low moment case [11]. Thus we expect $\langle |Z_{\Delta t}|^K \rangle \approx \Delta t^{K/\alpha} \langle |\tilde{Z}|^K \rangle$ to hold for lower moments. This means that the ratio $R(K, \Delta t) = \langle |S_{\Delta t}|^K \rangle / \langle |\tilde{S}|^K \rangle$ scales with Δt as $R(K, \Delta t) = \Delta t^{K/\alpha}$.

By using (6), (9), and (15), and considering the case with $K > \alpha$, l_{\max} finite, $\vartheta = 0$, and $\lambda_3 = 0$, we have for instance

$$E[|Z_{\Delta t}|^K] \approx \frac{\Delta t^{K/\alpha} 2\eta\Gamma(1+\alpha)\sin(\pi\alpha/2)}{\pi} O_{\text{damped}} \quad (22)$$

where

$$O_{\text{damped}} = \frac{l_{cs}^{(K-\alpha)}}{K-\alpha} + l_{ms}^{K-\alpha+\tau_1} e^{\lambda_1} \sum_{j \geq 0} \frac{\lambda_2^j}{j!} B_u(1+j\tau_2, K-\alpha+\tau_1) \quad (23)$$

and $l_{ms} = \Delta t^{-1/\alpha} l_{\max}$, $l_{cs} = \Delta t^{-1/\alpha} l_c$, and $B_u(1+j\tau_2, K-\alpha+\tau_1)$ is the incomplete Beta function with $1+j\tau_2 > 0$, $K-\alpha+\tau_1 > 0$, and $u = 1 - l_c/l_{\max}$. Thus the ratio $E[|Z_{\Delta t}|^K] / E[|Z_1|^K]$ is approximately given by

$$\Delta t^{K/\alpha} \frac{l_{cs}^{K-\alpha} + (K-\alpha)l_{ms}^{K-\alpha+\tau_1} e^{\lambda_1} \sum_{j \geq 0} \frac{\lambda_2^j}{j!} B_d(1+j\tau_2, K-\alpha+\tau_1)}{l_c^{(K-\alpha)} + (K-\alpha)l_{\max}^{K-\alpha+\tau_1} e^{\lambda_1} \sum_{j \geq 0} \frac{\lambda_2^j}{j!} B_d(1+j\tau_2, K-\alpha+\tau_1)} \quad (24)$$

In such a situation, the ratio $R(K, \Delta t)$ scales as $R(K, \Delta t) = \Delta t^{K/\alpha}$ if the ratio of (24) equals one. Nakao [11] previously noted that the self-similarity of $E_s[|Z_s|^K]$ breaks down if $K > \alpha$. If $K < \alpha$ then $E_s[|Z_s|^K] \approx E[|Z_1|^K]$; otherwise $E_s[|Z_s|^K] \neq E[|Z_1|^K]$. In practice the power law is of type $R(K, \Delta t) = v\Delta t^{K/\alpha}$ for some time interval Δt , where v is a constant describing the quasi-stable processes discussed in detail in Section 4. In such situations, ratio (24) gets approximately equal to v for $\Delta t_1 \leq \Delta t \leq \Delta t_2$. By depending solely on how the truncation parameters are set, a number of distinct scaling patterns can be uncovered. For example, if $l_c = 0$ then $E[|Z_{\Delta t}|^K]/E[|Z_1|^K] \approx \Delta t^{1-\tau_1/\alpha}$

The norm of the characteristic function can also be used to assess parameter γ by taking into account the same assumption that $P(Z_{\Delta t}) \approx L(Z_{\Delta t})$ for low values of $|K|$.

Since

$$\varphi(K) \equiv E[e^{iKZ_{\Delta t}}] = E[\cos(KZ_{\Delta t}) + i\sin(KZ_{\Delta t})] = E[\cos(KZ_{\Delta t})] + iE[\sin(KZ_{\Delta t})] \quad (25)$$

then the squared norm of $\varphi(K)$ is $\|\varphi(K)\|^2 = E^2[\cos(KZ_{\Delta t})] + E^2[\sin(KZ_{\Delta t})]$. For some K and Δt , $\|\varphi(K)\|$ can be estimated by

$$\|\hat{\varphi}(K)\|^2 = \langle \cos(KZ_{\Delta t}) \rangle^2 + \langle \sin(KZ_{\Delta t}) \rangle^2 \quad (26)$$

By assuming that $\ln[\varphi(K)] \approx -\gamma\Delta t|K|^\alpha$ for $0 < K < \alpha$, the “estimated” norm in logs of the characteristic function is $\ln\|\varphi(K)\|$, and then we can expect that $\ln\|\hat{\varphi}(K)\| = -\gamma\Delta t|K|^\alpha$.

Autocorrelations must be taken into account because of their effects on the characteristic function [8, 9]. Section 5 will show that for real-world currency data $\ln[\varphi(K)] \approx -\gamma\Delta t|K|^\alpha$ can occur, but only for tiny values of $K \in (0, k_0)$, where $k_0 \ll \alpha$.

4. Quasi-stable processes and multiscaling

Now consider a process with finite second moments. For “central variables”, i.e. $Z'_{\Delta t} = Z_{\Delta t} - \langle Z_{\Delta t} \rangle$ [8], the characteristic function can always be written as [2]

$$\varphi(K) = e^{-\sigma_{\Delta t}^2 K^2 (1 + w_{\Delta t}(\sigma_{\Delta t} K)) / 2} \quad (27)$$

where $w_{\Delta t}(0) = 0$. A “stable process” occurs whenever $w_{\Delta t}(K) = \text{constant}$ for all Δt within interval $\Delta t_1 \leq \Delta t \leq \Delta t_2$ [8]. But quasi-stable processes are more likely in practice where $w_{\Delta t}(K)$ is almost constant in the interval above. A “quasi-stable process” is similarly defined as $w_{\Delta t}(K) \approx \text{constant} \forall \Delta t_1 \leq \Delta t \leq \Delta t_2$. Some of us have shown [8] that a necessary condition for such a stability to occur is the presence of autocorrelations; otherwise $w_{\Delta t}(K) \rightarrow 0$ when $\Delta t \rightarrow \infty$ due to the central limit theorem.

Then we can show how multiscaling is related to the class of (quasi) stable processes. By expanding (27) we get

$$\ln \varphi(K) = 1 - \frac{1}{2} \sigma_{\Delta t}^2 K^2 + \frac{1}{3!} i^3 m_3 \sigma_{\Delta t}^3 K^3 + \frac{1}{4!} i^4 m_4 \sigma_{\Delta t}^4 K^4 + \dots + \frac{1}{p!} i^p m_p \sigma_{\Delta t}^p K^p + \dots \quad (28)$$

where every m_p is constant as required by the condition of stability. By definition we also have that

$$\psi_{\Delta t}(K) = 1 - \frac{1}{2} E[Z_{\Delta t}^2] K^2 + \frac{1}{3!} I^3 E[Z_{\Delta t}^3] K^3 + \frac{1}{4!} I^4 E[Z_{\Delta t}^4] K^4 + \dots + \frac{1}{p!} I^p E[Z_{\Delta t}^p] K^p + \dots \quad (29)$$

By comparing equal order terms in (28) and (29) we get

$$E[Z_{\Delta t}^p] = m_p \varpi \sigma_{\Delta t}^p \quad (30)$$

And if the autocorrelations are such that the second moment obeys a power law of type

$$\sigma_{\Delta t} = \varpi \Delta t^{1/\alpha} \quad (31)$$

where $\Delta t_1 \leq \Delta t \leq \Delta t_2$, then we have

$$E[Z_{\Delta t}^p] = m_p \varpi \Delta t^{p/\alpha} \quad (32)$$

Eq. (32) is thus in accordance with the results in Section 3.

Elsewhere [8] some of us showed that autocorrelations even at the noise level are compatible with scaling power law (31). Also, (31) together with the property of quasi-stability are sufficient for the emergence of the typical scaling in the probability of return to the origin of the TLF. Here analysis has been extended to encompass multiscaling.

5. Data and analysis

Now we are ready to assess the multiscaling properties in data coming from daily foreign exchange rates. The data sets employed were taken from the Federal Reserve website at <http://www.federalreserve.gov/releases/H10/hist/>. They refer to a currency value in US dollar terms. These exchange rates were collected by the Federal Reserve Bank of New York from a sample of market participants. They are noon buying rates in New York from cable transfers payable in the foreign currencies. As standard, here we ignore “holes” from weekends and holidays; analysis thus focuses on trading days. We take the historic values of 30 currencies from the website above. Since the series for the euro is too short, we have decided to take a *false* euro instead to get a longer series. We build the fictitious series for the euro by following a methodology put forward by Ausloos and Ivanova [16]. Table 1 shows the 31 currencies, historical time period, and number of data points.

As observed, we have already shown [8] that autocorrelations are related to the emergence of the TLF in such a data set. Parameters α and γ were estimated there by plotting $L(0)$ against Δt , where $L(0)$ is the probability of return to the origin for a given Δt . Alternatively, some of us have adopted a distinct parameter estimation practice [14] by using a maximum likelihood approach for α and γ together with nonlinear least squares for the other parameters. The estimates then turned out to be only slightly different.

Fig. 1 displays sample ratios $R(K, \Delta t)$ for several values of K in log-log plots of the exchange rates. Some ratios exhibit power law dependence on Δt . Pictures with lines which are dependent on K emerge in some of the plots.

By fitting $\log R(K, \Delta t) = \xi \log \Delta t$ for every K , we get the corresponding scaling exponents shown in Fig. 2. Some curves show linear dependence on K , for $0 < K < \alpha$. However scaling breaks down after $K > \alpha$, and a nonlinear behavior steps in.

For comparison we take our previous estimates of α . For Australia, α is equal to 1.415 and 1.4753 in [8] and [14] respectively. But at the first plot in Fig. 2 a linear behavior is found for $0 < K < 1.5$. After such an interval, the line gets constant. For Brazil, α is estimated to be equal to 0.8906 and 0.596 in [8] and [14] respectively. However an approximate linear behavior is here found for $0 < K < 3$. China provides an interesting exception, though. Here the linear behavior emerges for $0 < K < 1.0$. This seems at odds with the estimation of α greater than one found in [8].

The idiosyncratic behavior of the yuan has been assessed by some of us elsewhere [24]. Price changes of the yuan/dollar rate were found to display a Sierpinski triangle in an Iterative Function System clumpiness test. The Sierpinski triangle is a fractal structure that emerges commonly in “the chaos game”, where randomness coexists with deterministic rules. A threshold model with four states, two deterministic and two stochastic, was shown [24] to replicate these idiosyncratic features.

Fig. 3 displays the sample logarithm of the absolute characteristic function versus Δt for several values of K . A power law dependence on Δt seems again to emerge from the pictures.

By fitting $\ln\|\hat{\phi}(K)\| = \zeta\Delta t$ for every K , the estimated values of ζ versus $|K|^{\hat{\alpha}}$ are plotted in Fig. 4. Britain, Brazil and Canada show a linear dependence for all $K < 3$. For all the other cases, the linear dependence on the initial values of K are followed by nonlinear patterns.

Table 2 shows results for all currencies, where either single scaling or multiscaling is displayed in connection not only with exponent ξ but also with exponent ζ . As can be seen, multiscaling is pervasive among foreign exchange rates.

6. Conclusion

Whether scaling is single or multiple depends on how a Lévy flight is broken. While the abruptly truncated Lévy flight exhibits mere single scaling, the smoothly truncated one can show multiscaling [11, 15].

We have previously shown [8] that sharply truncated Lévy flights might prove to be suitable for describing daily exchange rate data. A novelty in this paper is to move up and show that such sort of data set also presents multiscaling if the sharp truncation is dropped. By using our previously suggested exponentially damped Lévy flight [14] we show that multiscaling is pervasive in the same set of data. Also, the exponentially damped Lévy flight can help to understand the broken self-similarity of the K^{th} absolute moment. The multiscaling stemming from the exponentially damped Lévy flight is related, too, to the class of quasi-stable processes previously put forward by some of us [8].

The finding that multiscaling seems to be pervasive among the 31 currencies studied strengthens the case for real-world relevance of the Lévy flights for modeling financial prices.

Table 1
Description of data sets.

Country	Currency	Time Period	Data Points
Australia	Australian Dollar	4Jan71 – 10Jan03	8025
Austria	Shilling	4Jan71 – 31Dec98	6999
Belgium	Belgian Franc	4Jan71 – 31Dec98	7013
Brazil	Real	2Jan95 – 10Jan03	2014
Britain	Pound	4Jan71 – 10Jan03	8032
Canada	Canadian Dollar	4Jan71 – 10Jan03	8038
China	Yuan	2Jan81 – 10Jan03	5471
Denmark	Krone	4Jan71 – 10Jan03	8031
Euro Area	False Euro	4Jan93 – 10Jan03	2521
Finland	Markka	4Jan71 – 31Dec98	6976
France	Franc	4Jan71 – 31Dec98	7021
Germany	Deutsche Mark	4Jan71 – 31Dec98	7021
Ireland	Pound	4Jan71 – 31Dec98	7021
India	Rupee	2Jan73 – 10Jan03	7525
Italy	Lira	4Jan71 – 31Dec98	7020
Japan	Yen	4Jan71 – 10Jan03	8026
Malaysia	Ringgit	4Jan71 – 10Jan03	8010
Mexico	Peso	8Nov93 – 10Jan03	2300
Netherlands	Guilder	4Jan71 – 31Dec98	7021
New Zealand	New Zealand Dollar	4Jan71 – 10Jan03	8016
Portugal	Escudo	2Jan73 – 31Dec98	6518
Singapore	Singapore Dollar	2Jan81 – 10Jan03	5531
South Africa	Rand	4Jan71 – 10Jan03	8005
South Korea	Won	13Apr81 – 10Jan03	5416
Spain	Peseta	2Jan73 – 31Dec98	6521
Sri Lanka	Rupee	2Jan73 – 10Jan03	7172
Sweden	Krona	4Jan71 – 10Jan03	8031
Switzerland	Swiss Franc	4Jan71 – 10Jan03	8032
Taiwan	Taiwan Dollar	30Oct83 – 10Jan03	4548
Thailand	Baht	2Jan81 – 10Jan03	5428
Venezuela	Bolivar	2Jan95 – 10Jan03	2013

Table 2

Single scaling and multiscaling in exchange rates.

An approximate linear behavior for all K (all $\kappa(\alpha) = |K|^\alpha$) gives evidence of mere single scaling. In turn, a linear behavior for initial values of $K < \alpha_0$ ($\kappa(\alpha) < \alpha_0$) followed by a nonlinear pattern after $K > \alpha_0$ ($\kappa(\alpha) > \alpha_0$) indicates the presence of multiscaling.

Country	Currency	Exponent ξ	Exponent ζ
Australia	Australian Dollar	Multiscaling (2)	Multiscaling (2)
Austria	Shilling	Multiscaling (1.8)	Single Scaling
Belgium	Belgian Franc	Single Scaling	Multiscaling (0.3)
Brazil	Real	Single Scaling	Single Scaling
Britain	Pound	Single Scaling	Single Scaling
Canada	Canadian Dollar	Single Scaling	Single Scaling
China	Yuan	Multiscaling (1)	Multiscaling (1)
Denmark	Krone	Multiscaling (2)	Single Scaling
Euro Area	False Euro	Multiscaling (2.2)	Single Scaling
Finland	Markka	Multiscaling (2.1)	Single Scaling
France	Franc	Multiscaling (2)	Single Scaling
Germany	Deutsche Mark	Multiscaling (2)	Single Scaling
Ireland	Pound	Multiscaling (2)	Single Scaling
India	Rupee	Multiscaling (2)	Multiscaling (1.4)
Italy	Lira	Multiscaling (2.5)	Multiscaling (0.1)
Japan	Yen	Multiscaling (2)	Multiscaling (0.25)
Malaysia	Ringgit	Multiscaling (1.8)	Multiscaling (2)
Mexico	Peso	Multiscaling (2)	Multiscaling (1.5)
Netherlands	Guilder	Multiscaling (2.5)	Single Scaling
New Zealand	New Zealand Dollar	Multiscaling (1.5)	Single Scaling
Portugal	Escudo	Multiscaling (2.5)	Multiscaling (0.2)
Singapore	Singapore Dollar	Multiscaling (2)	Single Scaling
South Africa	Rand	Multiscaling (1)	Multiscaling (2)
South Korea	Won	Multiscaling (1.5)	Multiscaling (2)
Spain	Peseta	Multiscaling (2)	Multiscaling (~0)
Sri Lanka	Rupee	Multiscaling (~0)	Multiscaling (~0)
Sweden	Krona	Multiscaling (2)	Multiscaling (3)
Switzerland	Swiss Franc	Multiscaling (2.5)	Single Scaling
Taiwan	Taiwan Dollar	Multiscaling (1.5)	Multiscaling (0.5)
Thailand	Baht	Multiscaling (~0)	Multiscaling (0.5)
Venezuela	Bolivar	Multiscaling (1)	Multiscaling (~0)

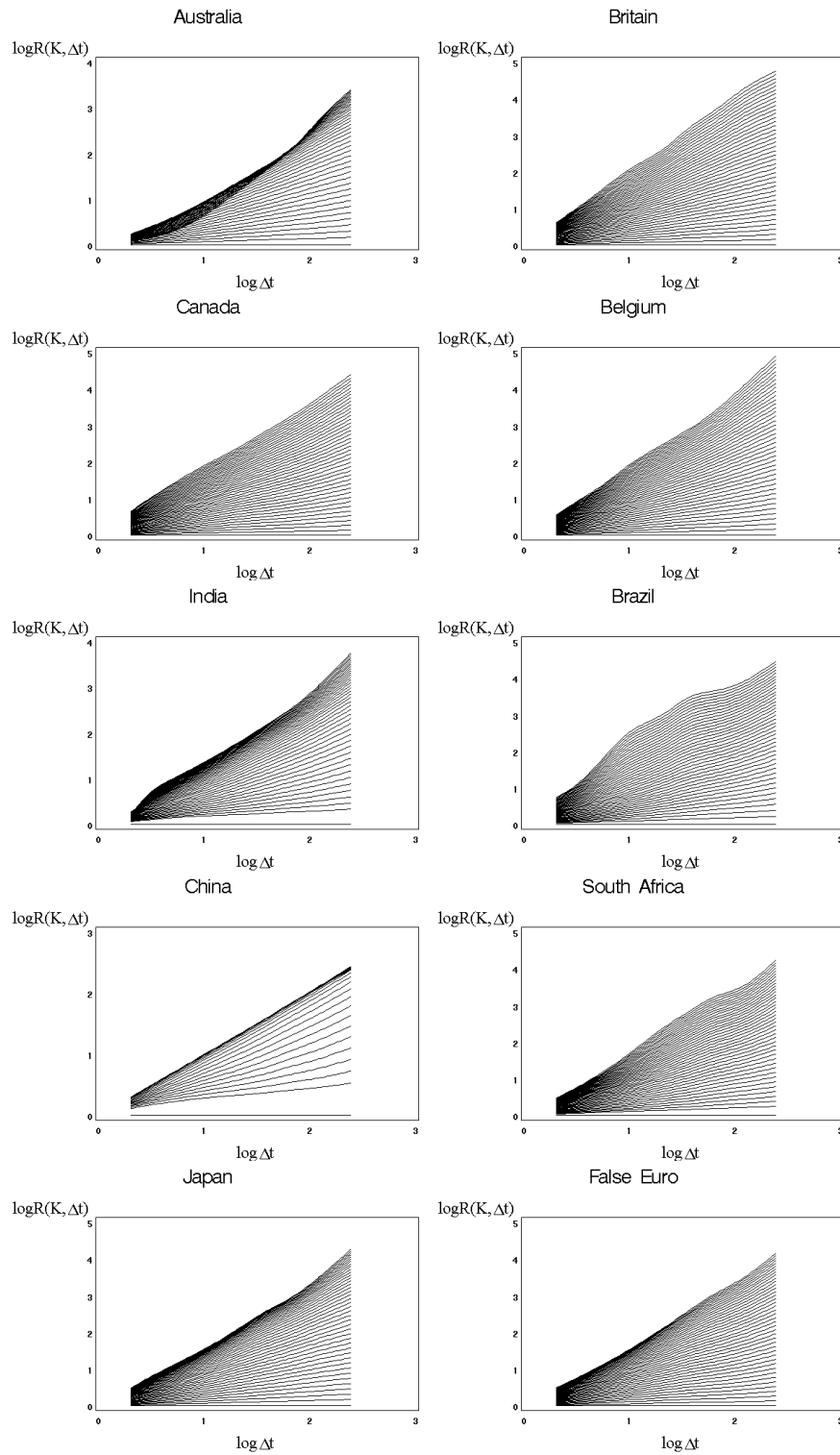


Fig.1. Estimated ratios $R(K, \Delta t)$ of selected exchange rates for $K = 0.0-3.0$ at intervals of 0.2. For each plot, the bottom line corresponds to $K = 0.0$, and the top one to $K = 3.0$.

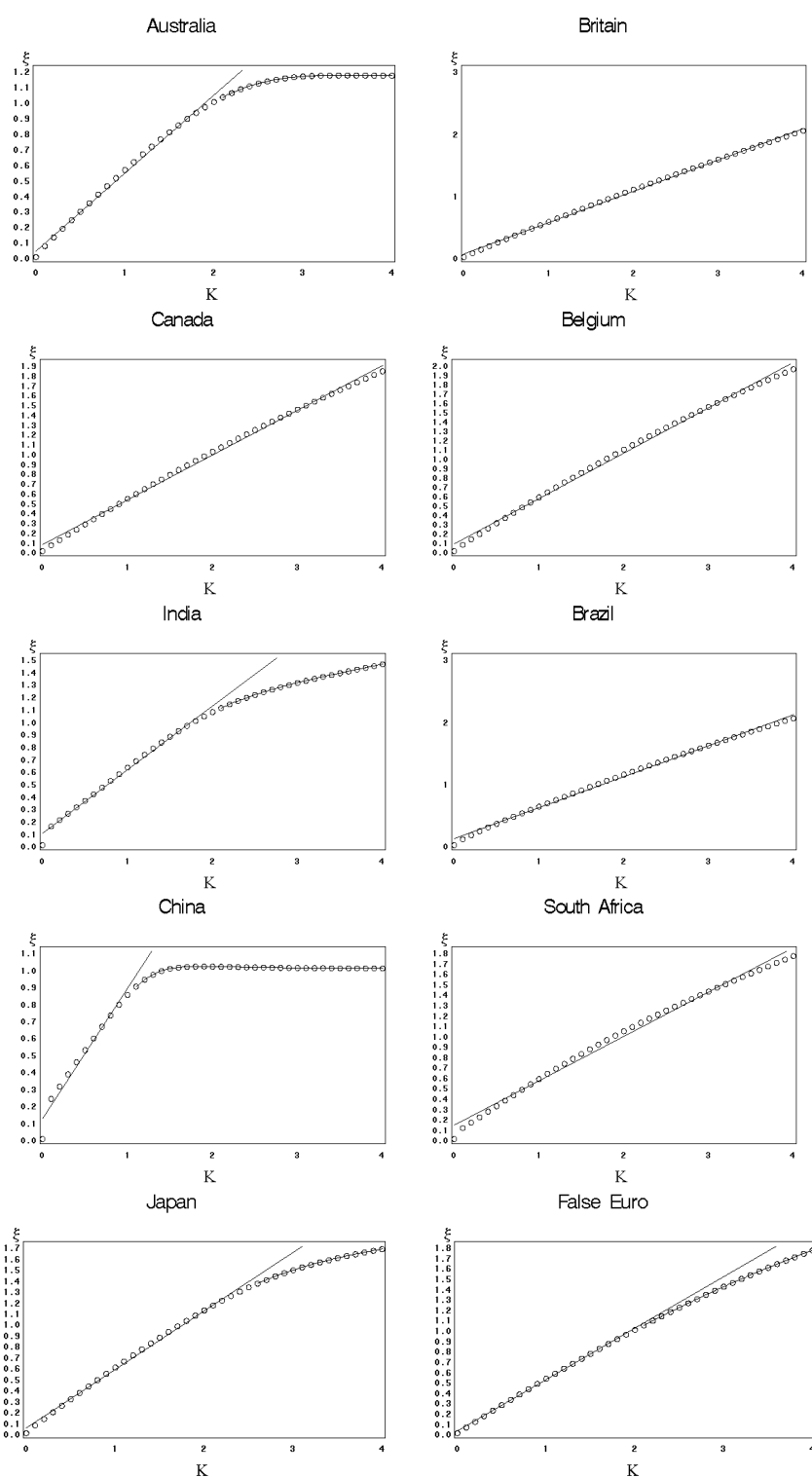


Fig.2. Estimated multiscaling exponents ξ for selected exchange rates. An approximate linear behavior for all K indicates mere single scaling. A linear behavior for initial values of $K < \alpha$ followed by a nonlinear pattern after $K > \alpha$ tracks the presence of multiscaling.

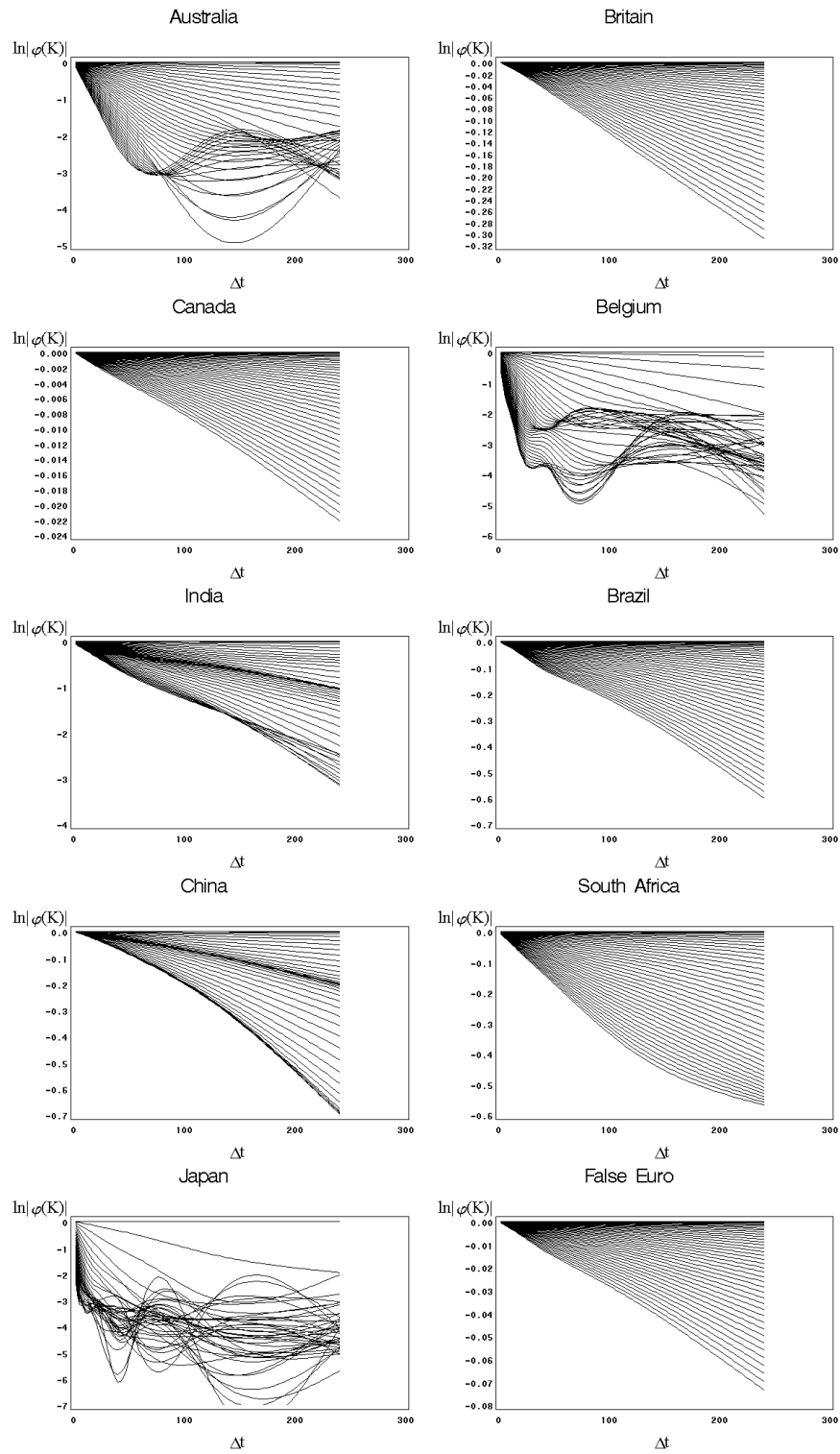


Fig.3. Estimated ratios $\ln|\varphi_L(K)|$ for selected exchange rates for $K = 0.0-3.0$ at intervals of 0.2. For each plot, the upper line corresponds to $K = 0.0$, and the bottom one to $K = 3.0$.

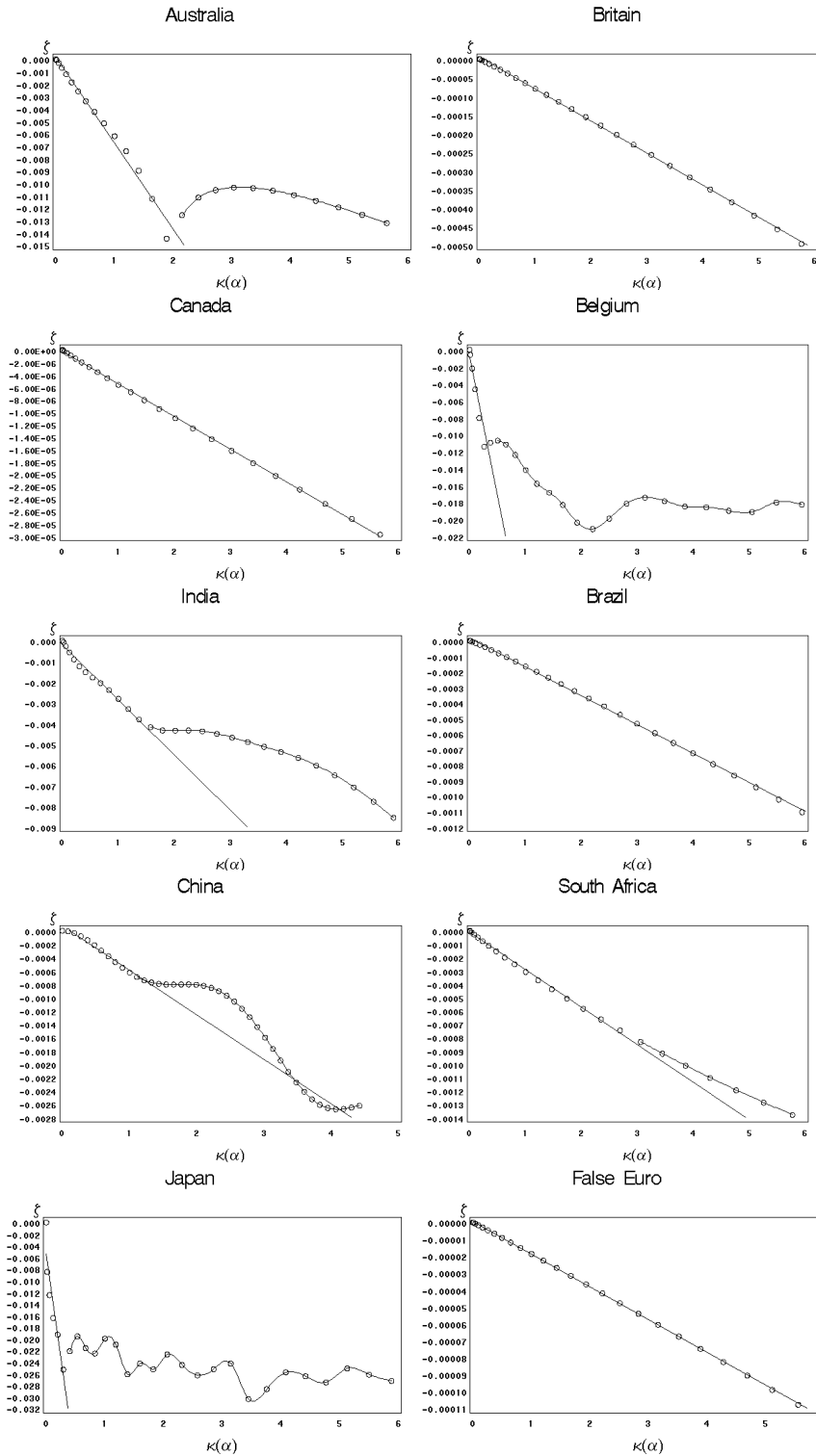


Fig.4. Estimated multiscaling exponents ζ for selected exchange rates. An approximate linear behavior for all $\kappa(\alpha) = |K|^\alpha$ indicates mere single scaling. A linear behavior for initial values of $\kappa(\alpha) < \alpha_0$ followed by a nonlinear pattern after $\kappa(\alpha) > \alpha_0$ tracks the presence of multiscaling.

References

- [1] A. Lo, A. C. MacKinlay, Stock market prices do not follow random walks: evidence from a simple specification test, *Rev. Fin. Stud.* 1 (1988) 41-66.
- [2] D. Dugué, *Oeuvres de Paul Lévy, Vol. III: Eléments Aléatoires*, Gauthiers-Villars, Paris, 1976.
- [3] B. B. Mandelbrot, The variation of certain speculative prices, *J. Business* 36 (1963) 394-419.
- [4] R. N. Mantegna, H. E. Stanley, Stochastic process with ultraslow convergence to a Gaussian: the truncated Lévy flight, *Phys. Rev. Lett.* 73 (1994) 2946-2949.
- [5] R. N. Mantegna, H. E. Stanley, Scaling behavior in the dynamics of an economic index, *Nature* 376 (1995) 46-49.
- [6] I. Gleria, R. Matsushita, S. Da Silva, Scaling power laws in the Sao Paulo Stock Exchange, *Econom. Bull.* 7 (2002) 1-12.
- [7] J. A. Skjeltorp, Scaling in the Norwegian stock market, *Physica* 283 (2001) 486-525.
- [8] A. Figueiredo, I. Gleria, R. Matsushita, S. Da Silva, Autocorrelation as a source of truncated Lévy flights in foreign exchange rates, *Physica A* 323 (2003) 601-625.
- [9] A. Figueiredo, I. Gleria, R. Matsushita, S. Da Silva, On the origins of truncated Lévy flights, *Phys. Lett. A* 315 (2003) 51-60.
- [10] I. Koponen, Analytic approach to the problem of convergence of truncated Lévy flights towards the Gaussian stochastic process, *Phys. Rev. E.* 52 (1995) 1197-1199.
- [11] H. Nakao, Multi-scaling properties of truncated Lévy flights, *Phys. Lett. A* 266 (2000) 282-289.
- [12] H.M. Gupta, J.R. Campanha, The gradually truncated Lévy flight for systems with power-law distributions, *Physica A* 268 (1999) 231-239.
- [13] H.M. Gupta, J.R. Campanha, The gradually truncated Lévy flight: stochastic process for complex systems, *Physica A* 275 (2000) 531-543.
- [14] R. Matsushita, P. Rathie, S. Da Silva, Exponentially damped Lévy flights, *Physica A* 326 (2003) 544-555.
- [15] B. Dubrulle, J. P. Laval, Truncated Lévy laws and 2D turbulence, *Eur. Phys. J. B* 4 (1998) 143-146.
- [16] M. Ausloos, K. Ivanova, Introducing false EUR and false EUR exchange rates, *Physica A* 286 (2000) 353-366.
- [17] N. Vandewalle, M. Ausloos, Multi-affine analysis of typical currency exchange rates, *Eur. Phys. J. B* 4 (1998) 257-261.
- [18] K. Ivanova, M. Ausloos, Low q-moment multifractal analysis of gold price, Dow-Jones industrial average and BGL-USD exchange rate, *Eur. Phys. J. B* 8 (1999) 665-669.
- [19] F. Schmitt, D. Schertzer, S. Lovejoy, Multifractal analysis of foreign exchange data, *Appl. Stoch. Model Data Anal.* 15 (1999) 29-53.
- [20] R. Gencay, F. Selcuk, B. Whitcher, Scaling properties of foreign exchange volatility, *Physica A* 289 (2001) 249-266.
- [21] Z. Xu, R. Gencay, Scaling, self-similarity and multifractality in FX markets, *Physica A* 323 (2003) 578-590.

[22] A. Bershanskii, Self-averaging phenomenon and multiscaling in Hong Kong stock market, *Physica A* 317 (2003) 591-596.

[23] R. Mantegna, H. E. Stanley, *An Introduction to Econophysics, Correlations and Complexity in Finance*, Cambridge University Press, Cambridge, 2000.

[24] R. Matsushita, I. Gleria, A. Figueiredo, S. Da Silva, Fractal structure in the Chinese yuan/US dollar rate, *Econom. Bull.* 7 (2003) 1-13.